J. Meas. Sci. Instrum., 2024, 15(2): 244-252.
DOI: 10.62756/jmsi.1674-8042.2024025
http://jmsi.publish.founderss.cn
jmsi@nuc.edu.cn

Adaptive compensation method for photomultiplier tube counting temperature drift

LI Gang, WANG Yaoqi*, WANG Xiaopeng

School of Electronic and Information Engineering, Lanzhou Jiaotong University, Lanzhou 730070, China

***Corresponding author:** WANG Yaoqi (wangyaoqi@lzjtu.edu.cn)

Received: October 11, 2023 **Revised:** December 4, 2023 **Accepted:** January 17, 2024

Abstract: The photomultiplier tube (PMT) is an important device for micro-light detection, and the detection of light intensity using photon counting method can significantly reduce the interference of noise, but the sensitivity, gain, and dark noise of PMT cathode are easily affected by the ambient temperature, which leads to the instability of the output pulse amplitude and affects the detection performance of the system for micro-light. A high voltage gain compensation and threshold correction system was designed for PMT through microcontroller unit (MCU), digital to analog converter (DAC), and other modules. A hybrid function model of temperature and high voltage compensation increment V_h and threshold compensation increment V_t was constructed by analyzing the cathode saturation current, sensitivity, and dark noise of PMT at different temperatures. And the compensation increment hybrid model was used to compensate the PMT counts output for adaptive temperature drift compensation. Experiments using this method with Hamamatsu's end-window PMT CR135 demonstrated that this system had a good output signal-to-noise ratio for large temperature variations, with an average count rate improvement of 0.19 at −20 ℃. Even though a small amount of dark noise was introduced, the detection performance was substantially improved.

Key words: photomultiplier tube (PMT); adaptive temperature drift compensation; compensated incremental hybrid model; cathode sensitivity

0 Introduction

The photomultiplier tubes (PMT) possess characteristics such as high sensitivity, low noise, and rapid response, making them the most suitable instruments for detecting visible, ultraviolet, and near-infrared radiation. They are used in a wide range of fields, including particle physics, nuclear physics, astronomy, and space science. PMT are crucial detectors in the realm of micro-light measurements, especially in the domain of extremely micro-light detection. They consist of several components, including an entrance window, a photocathode surface, a multiplication system, and an anode[1-6]. The photoelectrons generated by the external photoelectric effect are amplified by a gain of 10^5 times to 10^7 times through the photomultiplier tube, resulting in an anode current[7]. Due to the stochastic nature of secondary electron emission within the multiplication system, the current generated by each photoelectron at the anode is not fixed. Instead, the height of the current pulses follows a specific random distribution[8]. The PMTs are susceptible to environmental temperature variations. Decreasing temperatures lead to a reduction in cathode sensitivity and saturation current, resulting in a decrease in the height of electron current pulses output by the PMT. For photon counting, a valid photon count is determined by the threshold of the detector.

In practical applications, a fixed threshold is typically employed to extract valid signals, and the lower the threshold is set, the more comprehensive the signal extraction[9-11]. However, the photocathode and the various multiplication stages of the PMT are both subject to the influence of thermionic emission effects caused by environmental temperature variations. Therefore, when setting the threshold, the impact of dark noise needs to be taken into account[12-14]. Kapri et al.[15] proposed the optimal high voltage and temperature settings for PMT counting output. However, it does not consider how to ensure PMT performance at low temperatures. Feng et al.[16] designed a PMT control circuit board that used a computer to implement gain adjustment and temperature-adaptive adjustment of high voltage. But the impact of the identification threshold on PMT output do not be considered. Wang et al.[17] designed an automatic gain control circuit based on PMT, taking into account the characteristic of PMT gain changing with operating voltage. But the influence of temperature do not be considered.

The output gain of PMT is directly proportional to the supply high voltage. Consequently, it is possible to adaptively mitigate the influence of environmental temperature on PMT output performance through bidirectional compensation using high voltage increments and threshold calibration. Hamamatsu's end-window PMT, i.e., the CR135, was chosen to set up a micro-light detection counting system for temperature experiments and output testing. The study validated the effectiveness of a mixed function model, which included temperature and compensation increments (V_h and V_t), for adaptively compensating PMT counting output.

1 Theoretical analysis

1.1 Impact of temperature on probability of triggering photon events

The cathode saturation current has a linear relationship with temperature, and decreases with the increase of temperature. The cathode electron flow, after passing through the multiplication stages, generates current pulses at the anode, but the total gain μ of the current is not fixed.

According to Foord et al.[8], the secondary electron emission process in the first multiplication stage of the PMT follows the Poisson distribution. This process can be expressed as

$$P(n_1 = n) = \frac{\lambda^n}{n!}\exp(-\lambda), \tag{1}$$

where n_1 represents the number of electrons generated by the photoelectron after the first multiplication stage; λ_1 is the average value of the gain of the electron current pulses in the first multiplication stage. For each multiplication stage in a PMT, the quantity of generated electrons follows this distribution.

According to Woodward et al.[18] if gains λ of the r multiplication stages of the PMT are all the same, i.e., $\lambda = \lambda_1 = \lambda_2 = \cdots = \lambda_r$, and $\lambda \gg 1$, then the total system gain follows the Gaussian distribution. This process can be expressed as

$$G(n_r) \approx \frac{1}{\sqrt{2\pi}\,\delta_r}\exp\left[-\frac{(n_r - \lambda^r)^2}{2\delta_r^{\,2}}\right], \tag{2}$$

where $\delta_r = \lambda^{r-\frac{1}{2}}$. According to Eqs. (1) and (2), the probability distribution of pulse heights of the final gain output relative to the mean is shown in Fig.1.

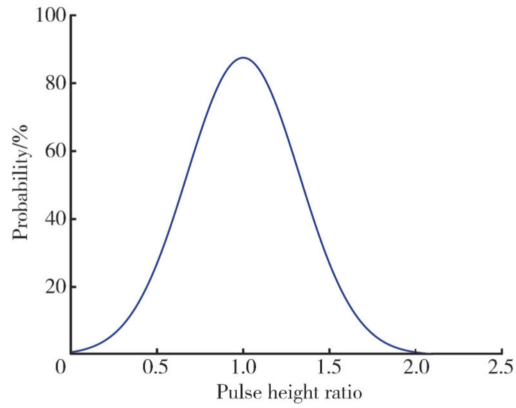

Fig. 1 Pulse height probability distribution of electron flow relative to mean from PMT output

The output voltage height, after passing through the $I-V$ circuit conversion, also followed the distribution.

When the environmental temperature decreases, the reduction in the number of electrons produced by the first multiplication stage is proportional to ρ. In the case where the gains $\lambda\rho$ of the r multiplication stages are the same, the system overall reduction in the total electron count is proportional to ρ^r. Under these conditions the total gain of the system can be approximated by a Gaussian distribution function and expressed as

$$G(n_r) \approx \frac{1}{\sqrt{2\pi}\,\delta_r}\exp\left[-\frac{(n_r - \rho^r\lambda^r)^2}{2\delta_r^{\,2}}\right], \tag{3}$$

where $\delta_r = (\rho\lambda)^{r-\frac{1}{2}}$. According to Eqs. (1) and (3), the probability distribution of the voltage heights of the final gain output of the PMT at different temperatures after passing through the $I-V$ conversion, relative to the mean value at room temperature, is shown in Fig.2.

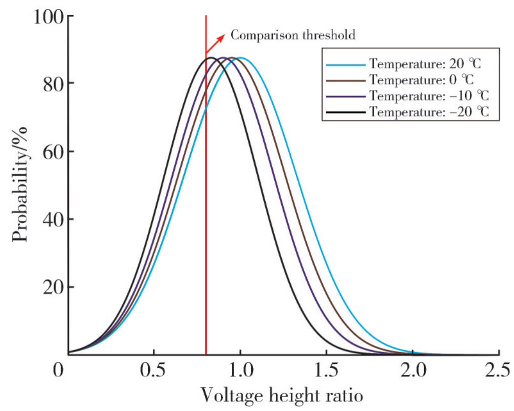

Fig. 2 Probability distribution of voltage height ratio at different temperature

When the set threshold remains constant, the probability of triggering photon events decreases as the temperature decreases, resulting in a decrease in the final PMT output count, thereby affecting the sensitivity of micro-light detection.

1.2 Influence of high voltage and threshold on count rate

The gain of the output pulses of the PMT was determined by the inter-stage voltages distributed to each multiplication stage due to the high voltage. Due to the influence of the electric field, the emission coefficient φ of photoelectrons was a function of the inter-stage voltage E[19], and can be expressed as

$$\varphi=\tau E^{k}, \tag{4}$$

where k is determined by the properties of the electrode itself and τ is a constant. The light-generated electron current I_k from the photocathode, under the influence of inter-stage voltage, impinges on the first multiplication stage plate, causing secondary electron emission and giving rise to the current I_1. The secondary electron emission coefficient φ_1 for the first multiplication stage can be expressed as[20]

$$\varphi_1=\frac{I_1}{I_{\mathrm{k}}}. \tag{5}$$

Assuming there are r multiplication stages in the PMT, when the photoelectrons pass through the nth ($1<n\leqslant r$) multiplication stage, the secondary electron emission coefficient φ_n can be expressed as[21]

$$\varphi_n=\frac{I_n}{I_{n-1}}. \tag{6}$$

By combining Eqs. (4), (5), and (6), the anode output current of the PMT after n multiplication stages of gain can be expressed as

$$I_{\mathrm{P}}=I_{\mathrm{k}}\xi\varphi_1\varphi_2\varphi_3\cdots\varphi_n, \tag{7}$$

where ξ is the electron collection efficiency. Then the current gain μ can be expressed as $\xi\varphi_1\varphi_2\varphi_3\cdots\varphi_n$.

When the gains of the r multiplication stages are the same, the relationship between the high voltage V and the current gain μ can be expressed as

$$\mu=\xi\left(\tau E^{k}\right)^{r}=\xi\tau^{r}\left(\frac{V}{r+1}\right)^{kr}=AV^{kr}, \tag{8}$$

where $A=\frac{\xi\tau^{r}}{(r+1)^{kr}}$. It can be inferred that the current gain is directly proportional to the krth power of the supply voltage V. Therefore, an increase in voltage will lead to a gain enhancement under ideal conditions. If identification threshold remains unchanged, the probability of triggering photon events will also increase.

However, increasing the voltage is accompanied by an increase in dark current, which is a faint current generated in the PMT due to issues like leakage current and thermionic emission in the absence of optical input. For PMT used in detecting micro-light, the increase in dark current leads to a decrease in the output signal-to-noise ratio, resulting in reduced detection sensitivity. The following discussion explores the main factors contributing to the generation of dark current. Because the materials used for the photocathode and multiplication stages of PMT have low work functions, thermal electron emission occurs even at room temperature, and the emission of thermal electrons is temperature-sensitive. The current due to thermal electron emission can be expressed as[22]

$$i_{\mathrm{s}}=AT^{\frac{5}{4}}\mathrm{e}^{-\frac{\Psi}{k_{\mathrm{B}}T}}, \tag{9}$$

where Ψ is the work function; T is the absolute temperature; e is the electron charge; and k_{B} is the Boltzmann constant. It is evident that the current due to thermal electron emission is a function of the photocathode surface and temperature, and the magnitude of the work function determines the quantity of thermal electron emission. When the cathode surface material is determined, it becomes a known factor, and in this case, temperature is the primary factor influencing current magnitude. A decrease in temperature results in a corresponding reduction in dark current, but lowering the temperature can only suppress dark current caused by thermal electron emission[23]. While thermal electrons are generated on both the photocathode surface and multiplication stages, the emission of thermal electrons is primarily determined by the photocathode surface because of its larger surface area and the lesser contribution of the subsequent multiplication stages to dark current. So, the impact of high voltage on the gain of dark current caused by thermal electron emission follows a similar trend to the change in current gain μ.

At lower temperature, the dark current caused by thermal electron emission was suppressed, and the proportion of leakage current generated by insulating materials was increased. It is independent of the current gain of the PMT and follows the Ohm's law.

It can be concluded that, under constant identification threshold conditions, the impact of temperature on the PMT output count rate can be compensated for by adjusting the high voltage. However, due to issues related to dark noise and the voltage output range of the high voltage module, increasing the supply voltage was not limitless. Too high power supply voltage will lead to the reduction of the output signal to noise ratio. Once the plateau voltage is reached, the balance between dark counts and counts generated by photoelectrons is achieved, marking the limit of the high voltage. The typical performance of the CR135 in temperature experiments confirms the aforementioned conclusion, as the PMT output count rate at different temperatures exhibits a linear relationship with the supply high voltage, as shown in Fig.3.

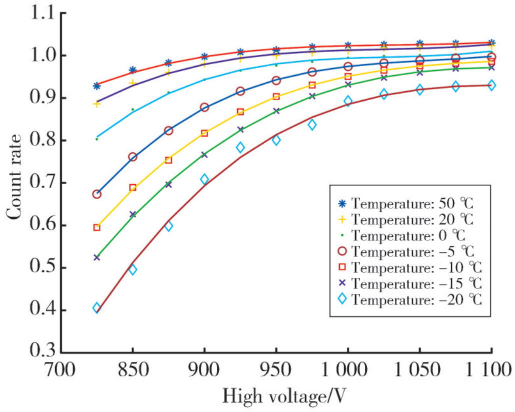

Fig. 3 PMT output count rate versus high voltage at different temperatures

In actual PMT use, it is not expected to operate at extremely high voltages. However, to ensure the stability of PMT operation, its operating voltage also needs to be positioned within the plateau region. In order to ensure both sufficient gain and stability for CR135 at different temperatures, the function for setting its high voltage should be expressed as

$$V = \theta_1 \exp(\theta_2 t) + \theta_3 \exp(\theta_4 t), \tag{10}$$

where θ_i is the offset factor, $\theta_1 = 4.443 \times 10^2$, $\theta_2 = -1.312 \times 10^{-2}$, $\theta_3 = 5.639 \times 10^2$, $\theta_4 = -3.734 \times 10^{-3}$. When using the plateau voltage of 950 V at room temperature (20 ℃) as a reference point, the high voltage compensation increment $V_h = V - 950$.

Because the gain adjustment due to the high voltage cannot completely offset the impact of temperature reduction on the PMT output count rate, it becomes necessary to adjust the identification threshold without increasing the influence of dark current on the count rate, in order to compensate for the remaining count loss. The main causes of dark current are thermal electron emission and leakage current. Therefore, combining Eqs. (8) and (9) with the Ohm's law, the anode dark current I_d can be expressed as

$$I_d \approx i_s \mu + i_e = A T^{\frac{5}{4}} e^{-\frac{\Psi}{k_B T}} V^{kr} + \frac{V}{R}. \tag{11}$$

After the $I-V$ conversion, the pulse amplitude of PMT dark count output was proportional to I_d, meaning $V_d \propto I_d$. Similarly, the pulse amplitude of count pulses generated by photon events was proportional to the anode output current, meaning $V_p \propto I_p$. If one intends to set the threshold V_1 in a way that it can filter out dark noise while maximizing the probability of triggering photon events, the threshold value should be expressed as

$$V_d \leqslant V_1 \leqslant V_p, I_d \chi \leqslant V_1 \leqslant I_p \chi,$$

$$\left(A T^{\frac{5}{4}} e^{-\frac{\Psi}{k_B T}} V^{kr} + \frac{V}{R} \right) \chi \leqslant V_1 \leqslant I_k A V^{kr} \chi, \tag{12}$$

where χ is the voltage conversion factor. When using the threshold V_0 at room temperature (20 ℃) as a reference point, the threshold compensation increment was $V_t = V_1 - V_0$. When their amplitudes overlap, the threshold value should be set at the intersection of the curve.

Due to the decrease in temperature, the reduction in the number of secondary electrons generated when photoelectrons collide with the multiplication stage plates results in a decrease in the amplitude of photon pulses. This leads to an overlap in size between the photoelectron flow and a portion of the anode leakage current. If high voltage is not adjusted and only the threshold is adjusted directly, it becomes impossible to distinguish between the two, causing a significant increase in the count of recognized pulses. Furthermore, the magnitude of anode leakage current is dependent on factors like plate materials and is uncontrollable, making it impossible to ensure system stability.

It can be inferred that both adjusting the high voltage and the threshold are compensation methods for PMT count rate drift. However, the individual action of either of them cannot achieve performance enhancement within the allowable error. It is necessary to first raise the high voltage to the plateau region, separating the anode leakage current from the photoelectron flow, and then perform threshold calibration to achieve effective temperature drift compensation. By incorporating the aforementioned temperature and high voltage compensation increment V_h and threshold compensation increment V_t hybrid function model into the microcontroller unit (MCU), it is possible to adaptively compensate for PMT count loss caused by temperature, ensuring enhanced performance.

2 Circuit design

2.1 System structure

The system structure block diagram is shown in Fig.4. The system was composed of CR135, STM32, high voltage power module, high-precision digital to analog converter (DAC), analog to digital converter (ADC), temperature sensor, operational amplifier, and other devices[24]. The core components consisted of the high voltage control compensation circuit and the threshold calibration circuit.

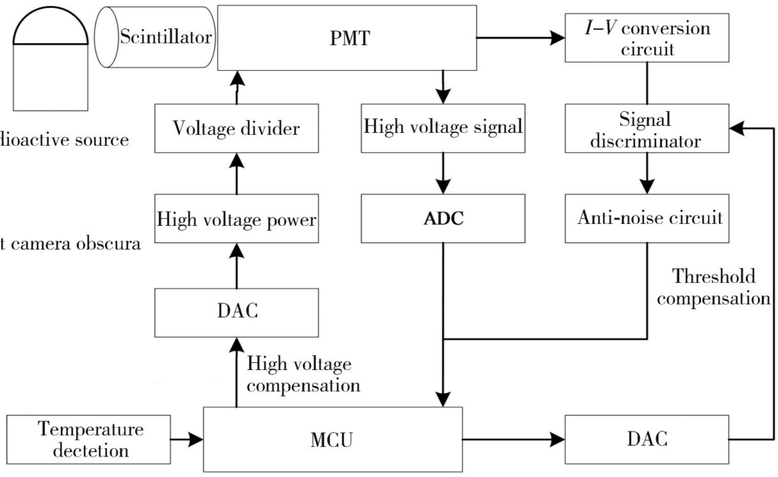

Fig. 4 System structure block diagram

The compensation process involved the PMT detecting the micro-light generated by a radiating scintillator, with the output photoelectron flow being converted into voltage and entering the discriminator. The signals that successfully triggered photon events were then shaped by the circuit before entering the MCU. When the temperature decreased, the MCU calculated the high voltage compensation increment V_h and threshold compensation increment V_t through the function model and sent them to the corresponding components via DAC to achieve the goal of adaptive compensation.

2.2 Core components

1) PMT

The adopted PMT was Hamamatsu CR135, known for its high gain and high collection efficiency, with detailed parameters as shown in Table 1. It was coupled with a NaI crystal scintillator, with the main emission peak around 415 nm. The used radioactive source was Cs-137.

Table 1 CR135 parameters

Parameter	Value
Spectral response range/nm	300—650
Photocathode materials	Dibasic
Glass shell material	Potassium-free borosilicate glass
Multiplication system structure	Box grid type
Stages	10
Cathode photo-sensitivity/(μA•lm^{-1})	60
Anode photo-sensitivity/(A•lm^{-1})	1 500
Dark current/nA	30

2) Threshold correction circuit

As shown in Fig. 5, this section utilized a 12-bit precision MCP4728 DAC chip for output the threshold compensation increment V_t. The pulse generated by the PMT output was negative concerning ground potential, and this signal entered the correction circuit through the IN terminal. In the absence of any light signal, the IN terminal high was pulled up by the static voltage on the feedback resistor of the PMT output. Meanwhile, the voltage at the positive input of the LM311 was higher than the negative input, resulting in a high-level output. When the photoelectrons were excited and eventually a stream of electrons were produced at the anode, the reverse voltage was superimposed on the feedback resistance through the output feedback resistance to the ground. This caused the voltage at the IN terminal to drop. The subsequent circuitry, isolated by a transistor, proportionally maintained the voltage at the IN terminal and fed it to the positive input of the LM311. If the voltage at the positive input was below a certain threshold, the comparator produced a low-level output. The method was based on the difference in signal amplitude to distinguish between dark noise and photon signals. By adjusting this threshold, the two could be distinguished.

In the STM32F103 microcontroller, the function model was executed to obtain the threshold increment V_t, which was transmitted to a DAC via the IIC protocol. Then, based on the threshold, the input signal was separated from the noise using a comparator constructed with LM311. This process ensured the probability of triggering a photon event.

3) High voltage compensation circuit

As shown in Fig.6, the used high voltage module was Hamamatsu's CC228P-01Y. By collecting the ambient temperature and calculating the high voltage compensation increment in STM32, the DAC chip interpreted commands and output corresponding control voltages to the V_{adj} pin to adjust the output high voltage value.

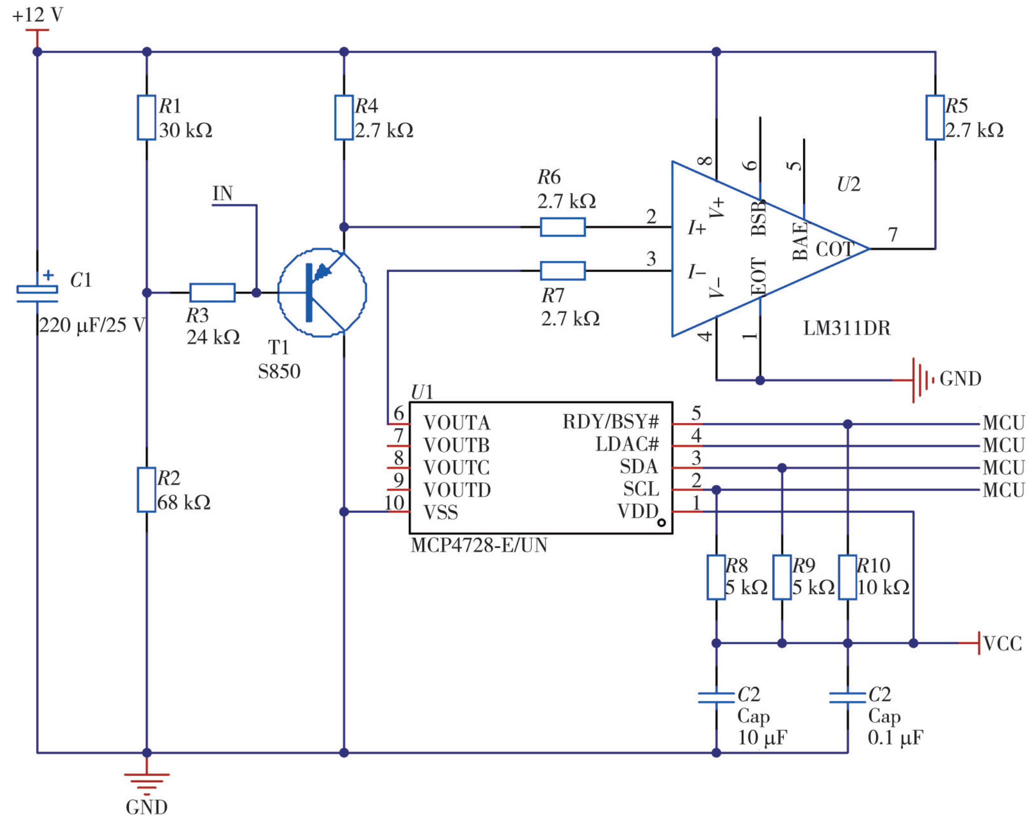

Fig. 5 Threshold correction circuit

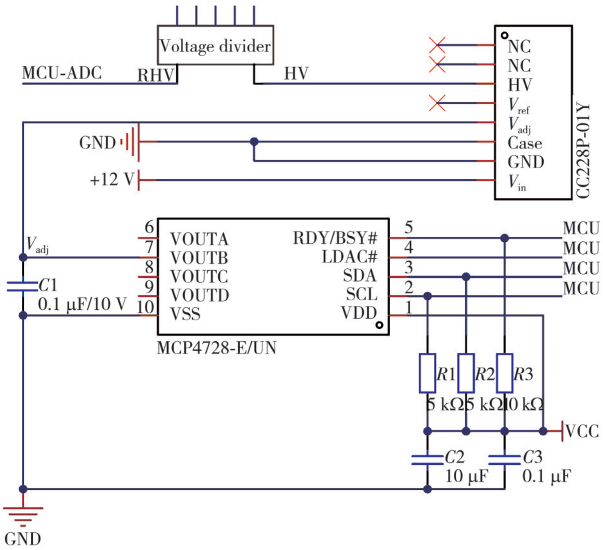

Fig. 6 High voltage compensation circuit

The high voltage was supplied to the PMT through a voltage divider and simultaneously fed back as the actual output high voltage value. Using the STM32 ADC pin, the feedback voltage was collected into the chip, compared with the desired compensation amount, and adaptively adjusted for control, reducing errors through a feedback mechanism to achieve precise compensation.

3 Experimental verification

The experimental setup was placed inside a constant temperature chamber, with the temperature set at 20 ℃ and a high voltage of 950 V. At this point, the CR135 exhibited dark noise amplitudes primarily concentrated around 100 mV. The discriminator threshold was set to 200 mV, and four sets of PMT from the same batch were prepared for a comparative experiment. The experimental setup's distance from the radiation source was kept constant, but the positions of each measurement device in every group were adjusted to place them at different radiation dose levels. Temperature adjustments were made in the temperature-controlled chamber at 5 ℃ intervals, starting from below 0 ℃.

The count rates of the four sets of devices at different experimental distances in response to temperature changes is shown in Fig. 7. When the identification threshold and high voltage gain remain constant, the triggering rate of photon events decreases continuously with decreasing temperature. At 0 ℃, the count rate loss was between 0.03 and 0.05, and when the temperature was dropped to −20 ℃, the count rate loss reached 0.1 to 0.3.

Even for the same device, due to varying intensities of the photoelectron pulse at different radiation distances and different intervals of signal amplitudes from the threshold, the reduction in photon event rate was different. At this point, the threshold was set above the average dark noise level, and lowering the temperature weakened the dark noise, so there was no need to consider the impact of dark counts on the system. When the count rate loss reached 0.1 or even 0.3, it could cause significant errors in the detection of micro-light intensities, leading to a loss of sensitivity in the system. Keeping the identification threshold constant, automatically compensating for the high voltage increment V_h was set in the MCU based on Eq. (10), raising the gain at different temperatures while avoiding the introduction of dark noise, and the final result is as shown in Fig.8.

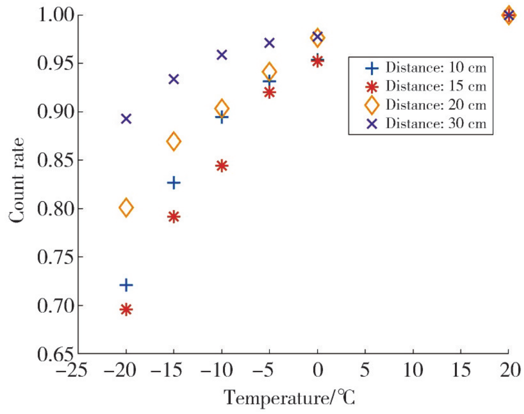

Fig. 7 Variation of count rate with temperature for four groups of devices at different distances

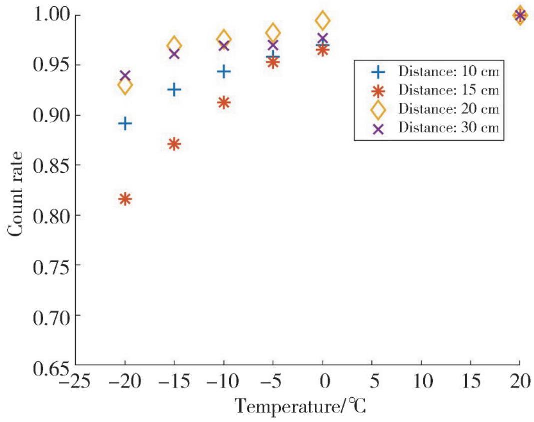

Fig. 8 Variation of count rate with temperature after adjusting voltage at different distances

Compensating for temperature-induced drift in the system output through high voltage gain adjustment without introducing dark noise was effective. At 0 ℃, the count rate loss ranged from 0.01 to 0.04 with an average improvement of 0.02. At −20 ℃, the count rate loss ranged from 0.06 to 0.18 with an average improvement of 0.12. However, the method had its limitations. Continuously increasing the high voltage will introduce dark counts, significantly increasing the probability of pulse pile-up events. Even though there might be some improvement visible in the system output, the uncertainty caused by pulse pile-up leaded to substantial variations in sensitivity and a sharp increase in instability when using the system at different time intervals. By keeping the initial high voltage constant and automatically adjusting the identification threshold V_t based on Eq. (12) within the MCU, the final output results at different temperatures is shown in Fig.9.

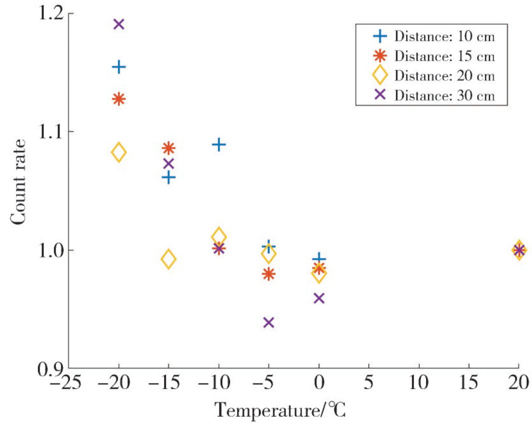

Fig. 9 Variation of count rate with temperature after adjusting threshold at different distances

If high voltage is not adjusted and the identification threshold is directly lowered, it will result in the inability to distinguish between the anode leakage current and the photoelectron flow. This leads to severe fluctuations in the count rate and the inability to find a corresponding pattern. At this point, the signal is superimposed with a significant amount of noise, rendering the system unable to operate in a stable state. Based on the adaptive adjustment of the high voltage, the identification threshold is automatically adjusted according to Eq. (12) within the MCU. The final triggering of photon events at different temperatures is shown in Fig.10.

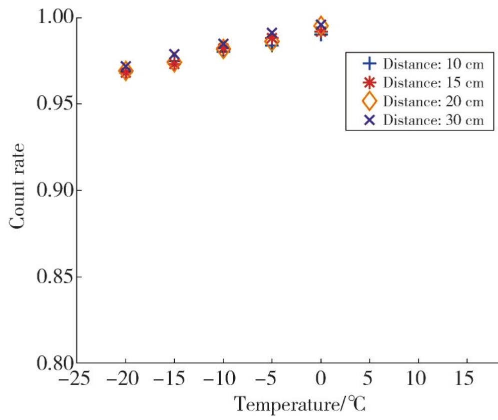

Fig. 10 Variation of count rate with temperature after adjusting voltage and threshold at different distances

The automatic setting of V_t can raise the output count rate of the PMT at different temperatures within the allowable range of system errors. The average count rate loss was 0.01 at 0 ℃ and 0.04 at −20 ℃. At this point, the identification threshold was typically set near the intersection of dark noise and photoelectron signal. If threshold voltage is further lowered, the probability of PMT being affected by noise photons will increase, leading to a decrease in the system output signal-to-noise ratio. Increasing the identification threshold, on the other hand, will lead to an overall decrease in the detection probability of photon events. As can be seen from Table 2, a small amount of dark noise is introduced by using this method. While it may not fully recover the detection sensitivity at room temperature, it effectively prevents the larger impact caused by increasing dark noise within an acceptable error range. Simultaneously, it allowed for noise background calibration in the software program, automatically filtering out dark counts at different temperatures, thereby reducing the adverse effects of this method.

Table 2 Comparison of dark noise for different methods

Methods	Dark noise/counts per second					
	20 ℃	0 ℃	−5 ℃	−10 ℃	−15 ℃	−20 ℃
Fixed threshold	546	438	362	229	188	156
High voltage compensation	546	443	369	241	203	164
Threshold compensation	546	459	386	307	272	228

As shown in Table 3, it is evident that compared to the traditional fixed threshold and supply voltage setting methods, this study can more effectively enhance the system output count rate at low temperatures. The experimental results showed that the adaptive compensation method was very effective to reduce the sensitivity of PMT at low temperature.

Table 3 Counts compensation rate at different temperatures

Compensation results	Counts compensation rate/%					
	20 ℃	0 ℃	−5 ℃	−10 ℃	−15 ℃	−20 ℃
Minimum	0	1.84	2.00	2.59	4.53	7.93
Mean	0	2.83	4.61	8.20	11.97	19.17
Maximum	0	3.98	6.75	13.78	18.13	27.21

4 Conclusions

Due to the sensitivity, gain, and dark noise sensitivity of the PMT cathode to ambient temperature, the output pulse amplitude became unstable, which adversely affected the performance of the system to detect low light. The use of fixed values made the system trigger photon events with different probabilities at different temperatures. The effects of noise and gain can reduce the sensitivity of the system to low light. To address the problem of temperature-induced count drift in PMT output, a hybrid function model was developed and experimental validation was conducted by using the CR135 to establish a micro-light detection counting system. The experimental results showed that although a small amount of dark noise was introduced at low temperatures, it increased the probability of triggering a photon event. At −20 ℃, the average output count rate was increased by 0.19, reaching a detection level comparable to that at room temperature within the acceptable error range. Therefore, the adaptive temperature drift compensation method proposed in this study was more suitable for the operation of PMT under different temperature conditions than the conventional method.

Acknowledgement

This work was supported by Gansu Province Higher Education Industry Support Plan Project (No.2023CYZC-40); Lanzhou Science and Technology Development Plan Project (No.2023-3-104).

Declaration of conflicting interests

The authors have no conflict of interests related to this publication.

References

[1] GHAHREMANI GOL M, KHAKZAD M, JAMILI S, et al. PMT glass window sensitivity to gamma-rays: a digital signal processing approach. Nuclear Instruments and Methods in Physics Research Section A: Accelerators, Spectrometers, Detectors and Associated Equipment, 2020, 957: 163401.

[2] LUO F, HENG Y, WANG Z, et al. A study of the new hemispherical 9-inch PMT. Journal of Instrumentation, 2019, 14(2): T02004.

[3] POPOV V, MAJEWSKI S, WOJTSEKHOWSKI B, et al. A simple method to increase effective PMT gain by amplifier circuit powered from voltage divider//2001 IEEE Nuclear Science Symposium Conference Record, November 4-10, 2001, San Diego, CA, USA. New York: IEEE, 2001: 634-637.

[4] NOWAK VEL NOWAKOWSKI P, MAKOWSKI D, MIELCZAREK A. Low-noise amplifier for photomultiplier tube detectors for plasma diagnostics//2021 28th International Conference on Mixed Design of Integrated Circuits and System, June 24-26, 2021, Lodz, Poland. New York: IEEE, 2021: 69-73.

[5] WANG W, JIANG Y, WANG C, et al. Research progress on detection of weak light signal by photomultiplier tube//2021 International Conference on Advanced Electrical Equipment and Reliable Operation, October 15-17, 2021, Beijing,

China. New York: IEEE, 2021: 1-5.

[6] KUANG W Z, WU M L, XU I. Dynamic obstacles detection of tram based on laser radar. Journal of Measurement Science and Instrumentation, 2018, 9(4): 316-320.

[7] FOORD R, JONES R, OLIVER C J, et al. The use of photomultiplier tubes for photon counting. Applied Optics, 1969, 8(10): 1975-1989.

[8] KITSMILLER V J, CAMPBELL C, O'SULLIVAN T D. Optimizing sensitivity and dynamic range of silicon photomultipliers for frequency-domain near infrared spectroscopy. Biomedical Optics Express, 2020, 11(9): 5373-5387.

[9] XIE G C, YE Y D, LI J M, et al. Echo characteristics and range error for pulse laser ranging. Chinese Journal of Lasers, 2018, 45(6): 260-267.

[10] XIA J, QIAN S, WANG W, et al. A performance evaluation system for photomultiplier tubes. Journal of Instrumentation, 2015, 10(3): 03023.

[11] WANG Y, CAO G, WEN L, et al. A new optical model for photomultiplier tubes. The European Physical Journal C, 2022, 82(4): 329.

[12] LEI X C, HENG Y K, QIAN S, et al. Evaluation of new large area PMT with high quantum efficiency. Chinese Physics C, 2016, 40(2): 026002.

[13] XIANG Y Y, LI S, MA Y. Effect of pile-up of electron flow pulse from photomultiplier tube on ranging by photon counting. Acta Physica Sinica, 2022, 71(21): 214206.

[14] LI Y, WANG L Q, HUANG Y, et al. Study on noise characteristics of photoelectric detection system and noise reduction design. Optics and Precision Engineering, 2020, 28(12): 2674-2683.

[15] KAPRI R K, RATHORE K, DUBEY P K, et al. Optimization of control parameters of PMT-based photon counting system. Mapan, 2020, 35(2): 177-182.

[16] FENG P, ZHANG Z Y, DING H B. Design and fabrication of control circuit for lidar PMT detection module. Journal of Atmospheric and Environmental Optics, 2022, 17(4): 465-475.

[17] WANG F, SUN K J, XIAGN X M. Research of automatic gain control technology based on photomultipliers. Laser Technology, 2015, 39(4): 510-514.

[18] WOODWARD P M. A statistical theory of cascade multiplication. Mathematical Proceedings of the Cambridge Philosophical Society, 1948, 44(3): 404-412.

[19] GUO L H, TIAN J S, LU Y, et al. Optimization of the 3-inch photomultiplier tube for the neutrino detection. Acta Physica Sinica, 2016, 65(22): 228501.

[20] YOU J W, ZHANG J F, LI Y, et al. Research and extension of Vaughan's secondary electron emission. High Power Laser and Particle Beams, 2013, 25(11): 3035-3039.

[21] CHANG T H, ZHENG J R. Monte-Carlo simulation of secondary electron emission from solid metal. Acta Physica Sinica, 2012, 61(24): 241401.

[22] ZUO Y H, WANG J G, FAN R Y. Influence of space charge effect on Nottingham effect in thermal field emission. Acta Physica Sinica, 2013, 62(24): 247901.

[23] ZHANG J, CHEN Y L, ZHANG L. Application of sine cosine algorithm-support vector regression on temperature compensation of MEMS shear stress sensor. Journal of Measurement Science and Instrumentation, 2023, 14(3): 263-269.

[24] ZHU Y, WANG W J, FU W. DC calibration signal generator based on STM32. Journal of Test and Measurement Technology, 2020, 34(5): 396-400.

光电倍增管计数温漂自适应补偿方法

李　岗，王耀琦*，王小鹏

兰州交通大学 电子与信息工程学院，甘肃 兰州 730070

摘　要：光电倍增管是微光探测的重要器件，使用光子计数法对光强进行检测可以大幅降低噪声的干扰，但光电倍增管的阴极灵敏度、增益及暗噪声易受环境温度的影响，导致输出脉冲幅值的不稳定，影响系统对微光的检测性能。本文通过使用微控制单元、数字模拟转换器等模块对光电倍增管设计了高压增益补偿和阈值校正系统，通过对不同温度下光电倍增管的阴极饱和电流、灵敏度和暗噪声的综合分析，构建温度与高压补偿增量 V_h 及阈值补偿增量 V_t 混合函数模型，使用补偿增量混合模型对光电倍增管计数输出进行自适应温漂补偿。对滨松的端窗型光电倍增管CR135进行实验，证明了此系统在较大温度变化下仍具有良好的输出信噪比，在−20 ℃时计数率平均提升0.19，即使引入了少量暗噪声，仍大幅提升了探测性能。

关键词：光电倍增管；自适应温漂补偿；补偿增量混合模型；阴极灵敏度

引用格式：LI Gang, WANG Yaoqi, WANG Xiaopeng. Adaptive compensation method for photomultiplier tube counting temperature drift. Journal of Measurement Science and Instrumentation, 2024, 15(2): 244-252.